Improvement and unification of input images for photogrammetric reconstruction

Krzysztof Skabek, Piotr Łabędź, Paweł Ozimek

Institute of Computer Science
Cracow University of Technology
Warszawska 24, 31-155 Cracow, Poland
e-mail: kskabek@pk.edu.pl, plabedz@pk.edu.pl, ozimek@pk.edu.pl

In this paper, we compare techniques for 3D reconstruction from images. We focus on the pre-processing step of reconstruction: improving the input images. Several image processing algorithms are selected and tested.

The main goal is to improve the quality of the resulting 3D reconstruction. We use two approaches to analyze the 3D model fitting: comparing them to the orthophotomap and measuring the position among 3D reconstructions.

Keywords: computer vision, photogrammetric reconstruction, image processing.

1. INTRODUCTION

Photogrammetric reconstruction consists of retrieving the position and spatial relations among 3D points of the observed surface based on 2D photographs. Two elements are required for photogrammetric reconstruction: (1) a series of photographs and (2) reconstruction routines. Reconstruction routines consist of: (1) detection of key-points in photographs, (2) determination of spatial relations between them, (3) approximation of the key-points with a dense cloud of points and (4) fitting a triangular topology to it.

Such an approach is known in the literature as structure from motion (SfM) [4]. The popular and still developing application of this method is connected with unmanned aerial vehicles (UAV) [2]. The significant problem in photogrammetry is sufficient feature detection in images. Interesting ways to improve this process were proposed in [1].

The selection of photographs is a preliminary and extremely important stage in the reconstruction process. It is necessary to ensure high contrast and variety of colors in photographs, as it has a significant impact on the number and accuracy of the determined key-points.

The aim of this article is to study the application of image enhancements to improve the 3D reconstruction. We tested several image processing methods: converting into grayscale (GRAY), histogram stretching (HS), histogram equalizing (HE), adaptive histogram equalizing (AHE) and exact histogram matching (EHM).

2. TECHNIQUES OF PHOTOGRAMMETRIC RECONSTRUCTION

The suggested strategy of obtaining images for photogrammetric reconstruction is to focus only on a significant part of the scene and take a series of photographs around it at regular intervals.

Reconstruction becomes possible when corresponding points are found in at least two views. Therefore, the required overlap in adjacent photos is estimated at 60% coverage at the back and 80% coverage at the front.

It is not necessary to place the entire object in the field of view. It is enough to place its parts in neighbouring pictures with sufficient overlap. In order to obtain good reconstruction quality, it is necessary to ensure good lighting of the scene and avoid changing it. Light reflections appearing on the material are undesirable. Also, using flashlights and the presence of light sources in the field of view are undesirable.

A drawback of the photogrammetric technique is the imprecise reproduction of the scale. There are some ways to solve this problem, e.g., (1) by applying markers, gauges or objects of known dimensions in the reconstructed area, or (2) in case of aerial photography, it is possible to use georeferencing in the form of ground control points (GCPs).

3. Methods

As the input data, we used images taken with the DSLR camera. The photographs were taken with the use of automatic mode. For this reason, the main object visible on some of them was over- or underexposed due to the different light conditions. The difference in exposure causes problems with the proper work of the algorithm responsible for the reconstruction. To solve this inconvenience, we tested several image processing algorithms to improve the exposure and general contrast of the input images in order to improve the quality of the resulting 3D reconstruction.

As a base for the tests, images converted into the grayscale mode were used. The first algorithm that was used is a well-known histogram stretching method that maps the intensity values of the image into new values (generally full range of values that the image allows in current mode), as presented in Fig. 1b.

The second used image enhancement algorithm was the histogram equalization technique. This technique equalizes the gray levels in the image in the way that the histogram is as flat as possible so that the resulting gray levels would have similar numbers of pixels (Fig. 1c). After that operation, the cumulative histogram should have linear features.

Adaptive histogram equalization was the third method that was tried in order to enhance the images. This method differs from ordinary histogram equalization in the respect that the adaptive method (AHE) operates on small regions of the image instead of the entire image [6]. The transformation function for each pixel is calculated basing on a neighbourhood, whose size is one of the algorithm's parameters. Due to the fact that AHE tends to overamplify the contrast (and so the noise) the contrast-limited adaptive histogram equalization (CLAHE) algorithm was used instead. CLAHE limits contrast amplification in the way that it truncates the histogram at the predefined value, especially in homogeneous areas [8]. The transformed neighbouring tiles are combined afterward with the use of bilinear interpolation in order to avoid introducing image artifacts. The resulting image and its histogram differs significantly from the image obtained with the use of the ordinary histogram equalization technique (Fig. 1d).

Input: I – image
divide I into regions r
for *each $r \in I$* **do**
    calculate histogram
    clip histogram
    calculate the cumulative distribution function of pixel values
    map histogram
end
combine r using bilinear interpolation
return I_t – *transformed image*

Algorithm 1: Adaptive histogram equalization.
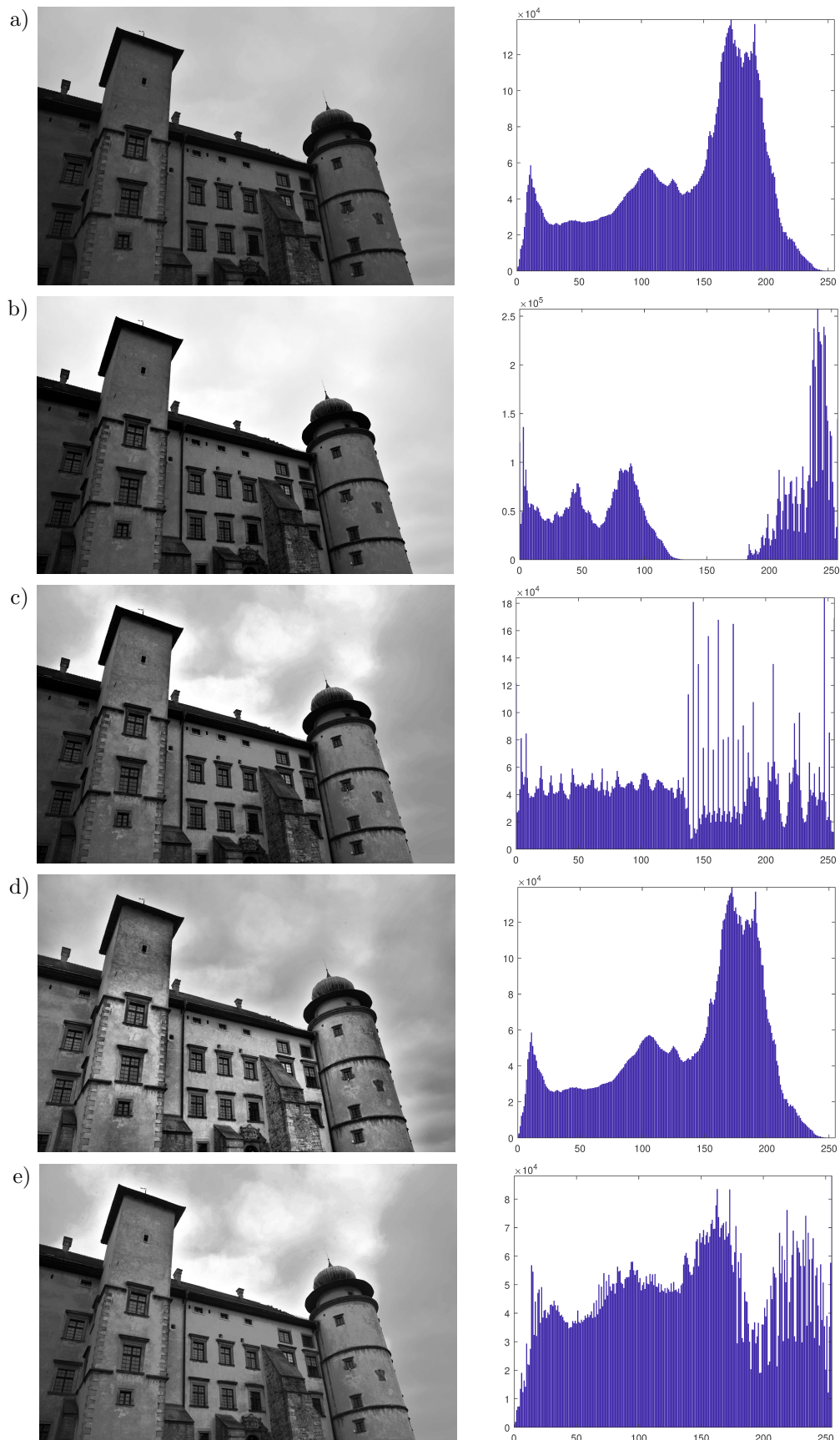
Fig. 1. Preprocessed images and their histograms: a) grayscale image (GRAY), b) histogram stretching (HS), c) histogram equalizing (HE), d) adaptive histogram equalizing (AHE), e) exact histogram matching (EHM).

The last image enhancement process consists of two main steps. In the first one, an average histogram of the whole set of images was calculated – histograms of each image were summed up and divided by a number of images in the set. In the second step, the obtained histogram was used to modify the images with the use of exact histogram matching operation [3, 7]. Each image was transformed in order to match the calculated average histogram (Fig. 1e).

Input: I_s – image set
for *each $I \in I_s$* **do**
  | calculate histogram I_h
end
calculate the average value of $I_h = I_{avg}$
for *each $I \in I_s$* **do**
  | transform I_h to match I_{avg}
end
return I_{st} – *transformed image set*

Algorithm 2: Exact histogram matching.

4. RESEARCH

Our research focused on the determination of whether the image enhancement has an influence on the resulting 3D model obtained by photogrammetric reconstruction. In order to perform such reconstruction, a set of photographs of the analyzed object should be obtained. In the presented, case the whole set of selected images consists of 158 photographs, and about 20% of them were underexposed. To enable modifications, they were converted into a grayscale mode and processed according to one of the mentioned methods. These sets of preprocessed photographs served as the input data to photogrammetric reconstruction performed by the certain program.

After performing photogrammetric reconstruction, the main type of data that is obtained is the sparse point cloud. It could be expanded into a dense point cloud through a separate process. The number of points in the sparse point cloud could be treated as one of the indicators describing the quality of the obtained cloud. The resulting number of points according to the used algorithms are presented in Table 1.

Table 1. Comparison of the number of points in the obtained sparse point cloud after using different image enhancement methods.

Used algorithm	Number of points in the sparse cloud
None (GRAY)	73 685
Histogram stretching (HS)	68 354
Histogram equalizing (HE)	72 073
Adaptive histogram equalizing (AHE)	83 637
Exact histogram matching (EHM)	98 713

Based on the sparse point clouds, the dense point clouds were created afterward. For each cloud generation, the same amount of images were taken. For each image, the depth map was calculated based on the estimated camera position and then combined into one dense cloud. Software used for this purpose created very dense clouds, with the number of points around 20 million. The reconstruction obtained with the use of unprocessed images is presented in Fig. 2.

Some major errors of the resulting reconstruction are clearly visible. The whole point cloud seems to consist of two separate parts. One of them is inclined at a certain angle to the other and breaks the entire model causing the whole reconstruction to be useless.
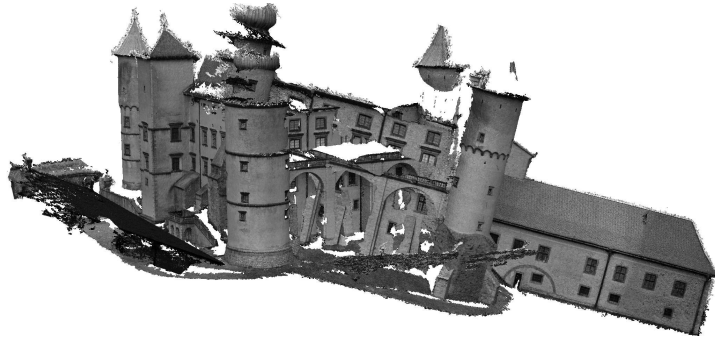
Fig. 2. Reconstruction performed with the use of original (grayscale) images.

The same problems are presented in the reconstruction created with the use of images that have been processed with the use of histogram stretching (Fig. 3). The point cloud seems to consist of two separate parts, and one of them is inclined to the other, but at a different angle and in a different place in the space.
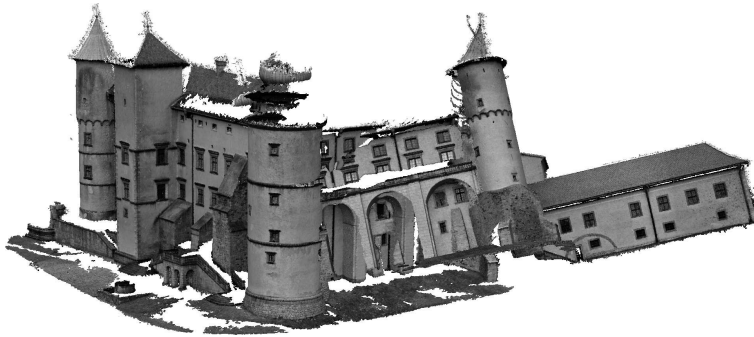
Fig. 3. Reconstruction performed with the use of images after histogram stretching.

Fig. 4. Reconstruction performed with the use of images after histogram equalizing.

Fig. 5. Reconstruction performed with the use of images after adaptive histogram equalizing.
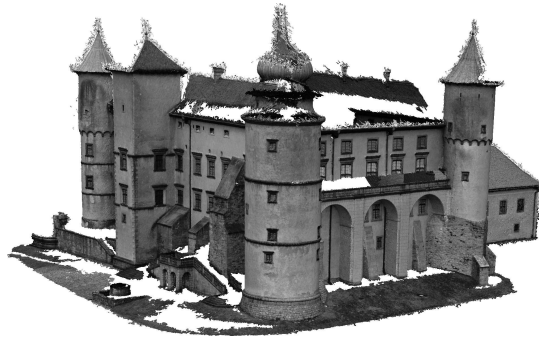
Fig. 6. Reconstruction performed with the use of images after exact histogram matching.

5. Comparison of 3D reconstruction quality

Based on the 3D reconstruction from the preprocessed set of input photographs, a comparison of the reconstruction quality was performed. This comparison was carried out in two stages: (1) an objective approach – using external data to measure and embed the processed model and (2) a relative approach – carried out to show the differences among the obtained 3D models.

In the objective approach, we used external data in the form of the orthophotomap from the online Geoportal (http://mapy.geoportal.gov.pl). Embedding the model on the map was done using GIS software. At this stage, the tested 3D models were embedded in the contour of the orthophotomap. In this way, information about the best model matching and its scale was obtained. The adjustment was done manually, taking into account the ground level and the height values of the models marked on the map with the appropriate colors from green (low altitude) to red (high altitude) in Fig. 7. As a result of matching, one best-fitting 3D model was selected – model AHE (M_{AHE}). This model was then used as a reference model to estimate the scale and to register the remaining reconstructions.

Fig. 7. Digital model embedded in the orthophotomap to check the correctness of its proportions.

In order to determine the scale, several measurements of significant distances were made within the base of the building reconstruction, and then the same distances were measured on the terrain surface on the map. The average ratio of these distances gave the estimation of the scale of the model. Other models were scaled against the reference model. The determination of the scale was performed together with the registration of individual reconstructions to the reference model.

The registration of the remaining models was the main task of the second stage of the model comparison process. For this purpose, the ICP method [5] was used for registration of relative sets of points and calculation of geometric transformation parameters: translation $\mathbf{T}$, rotation $\mathbf{R}$ and the scale $\mathbf{S}$. The isotropic character of the scale factor was assumed. The CloudCompare software was the programming base of the registration process. The manual registration routine was used where the operator appoints the pairs of characteristic points within the fixed and unchanging areas of the registered reconstructions.

Further part of the comparison consisted in determining the distance distribution of points for the obtained models to the reference AHE model. This was done in CloudCompare software using oct-trees (cloud-cloud distance). The distributions for particular models are shown in Fig. 8, where blue color means good fitting, green – weak fitting and red – no match.

a)   b)

c)   d)

e)
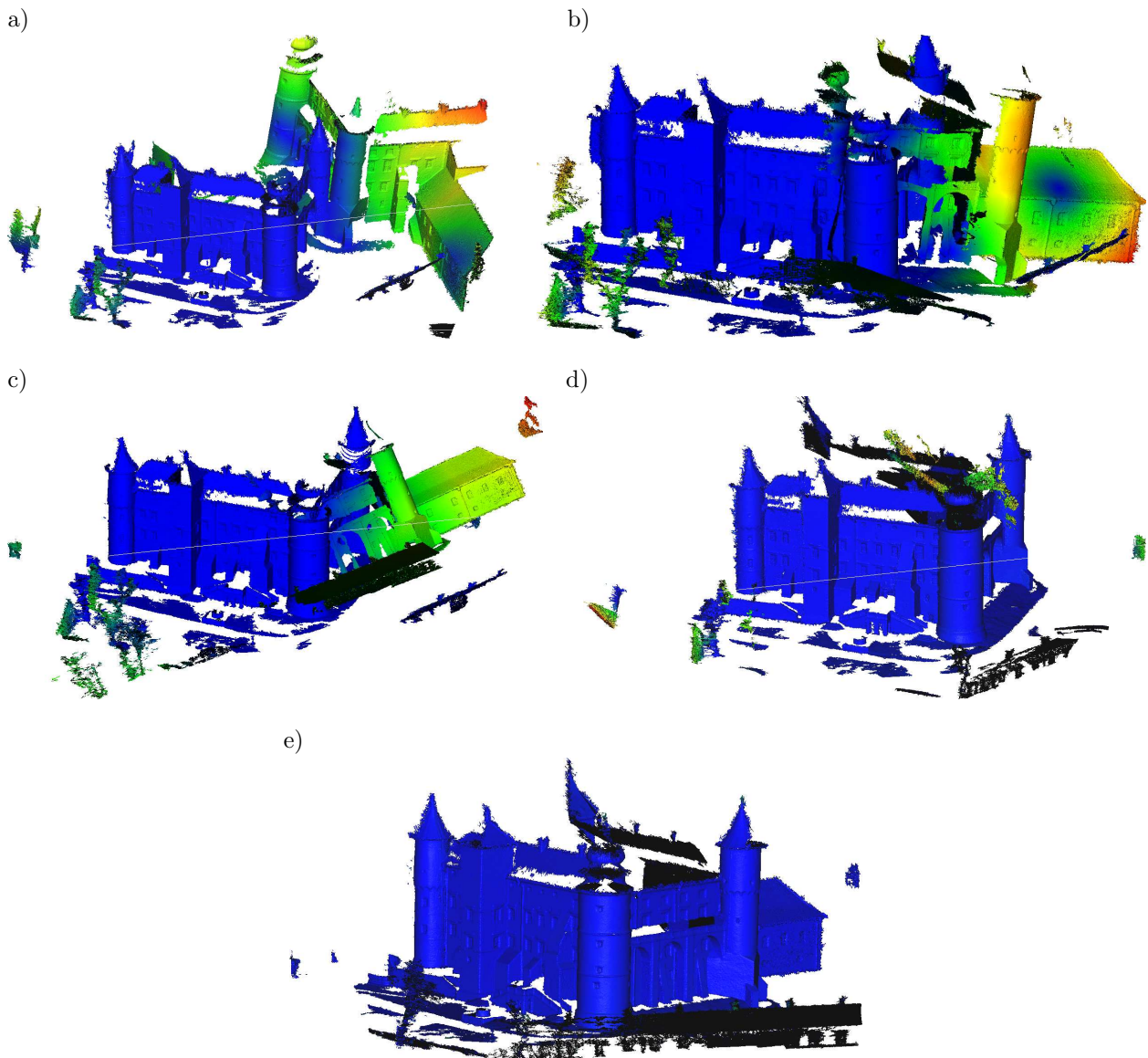
Fig. 8. Comparison of 3D reconstructions from differently preprocessed images to the reconstruction with AHE: a) original RGB images, b) images converted to grayscale, c) histogram stretching (HS), d) histogram equalizing (HE), e) exact histogram matching (EHM).

The quantitive comparison is given in Table 2. The values of mean distances and standard deviation for individual models in relation to the AHE reference model were included there. The

Table 2. Comparison of reconstructions (reference: reconstruction with AHE, V_{AHE} = 20 211 853 pts).

Reconstruction	Mean dist.	Std dev.	Dense cloud V_{dense}	Common vertices V_{comm} (d_{th} = 10 cm)	Common vertices V_{comm} (d_{th} = 1 m)
Original RGB	5.907	7.910	24 825 297	11 401 637	12 971 573
GRAY	3.476	4.800	21 384 710	3 451 337	12 373 399
HS	4.077	6.672	21 013 941	10 613 149	13 361 143
HE	0.230	0.720	14 333 996	5 516 522	14 142 654
EHM	0.119	0.323	21 143 778	14 205 884	20 903 091

sets of common points for the compared models were also determined assuming the threshold values d_{th} at the level of 10 cm and 1 m.

5.1. Summary of the comparison

In the reconstruction process, dense point clouds with a comparable number of vertices were obtained. It was approximately 20–24 Mpts. 14.3 Mpts were reconstructed in the model for which a significant decrease in the number of vertices was obtained by the HE method.

The best fit at the stage of the objective comparison with the orthophotomap was obtained by the AHE model (Fig. 11). When compared with the AHE reference model, the convergence of mean distances with the EHM and AHE models was visible. Therefore, considering the comparable complexity of these models, this allows to conclude on the similarity of the quality of EHM and AHE reconstruction methods. On the other hand, HE reconstruction allowed to obtain only 65% of points acquired by other methods.

The quality of model coverage was also examined (Table 2). For the EHM and AHE models, a coverage convergence of 98% was achieved with the assumed threshold distance d_{th} = 1 m and 67% for the threshold distance d_{th} = 10 cm. In the case of reconstruction using primary RGB images, these values were 52% and 46%, respectively.

6. ANOTHER TEST

In order to verify achieved results, another test on a different building was performed. Performing the reconstruction was much more difficult in this case as of the total number of 81 photos, 27% was underexposed and 10% overexposed. An additional difficulty was the fact that the solid of the building was very uniform with many repetitive elements, unlike in the case of the previously presented castle. Also, in this case, the worst reconstruction was generated from photographs without any pre-processing (Fig. 9). On two obtained reconstructions, only a fragment of the building's
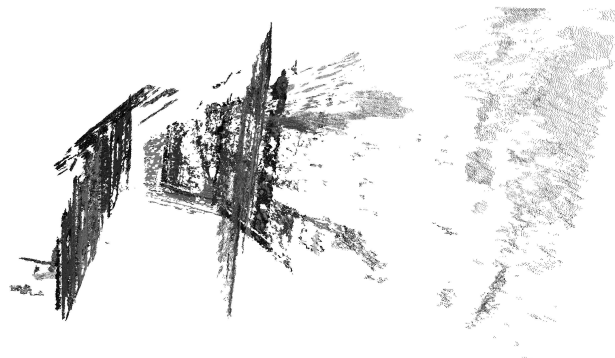
Fig. 9. Reconstruction performed with the use of original (grayscale) images.

body is visible (Figs 11 and 12). The probable reason is that the boundary photo in which the fragments of the front and sidewalls were included was underexposed, which caused the correct generation of only one sidewall that was photographed first. It is possible that a manual indica-

Fig. 10. Reconstruction performed with the use of images after histogram stretching.
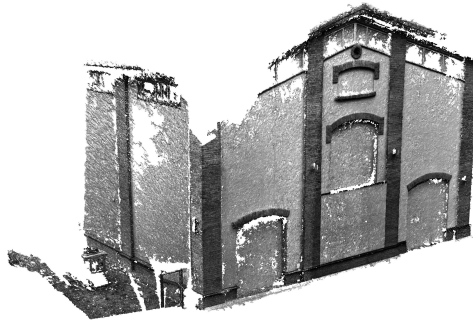
Fig. 11. Reconstruction performed with the use of images after histogram equalizing.
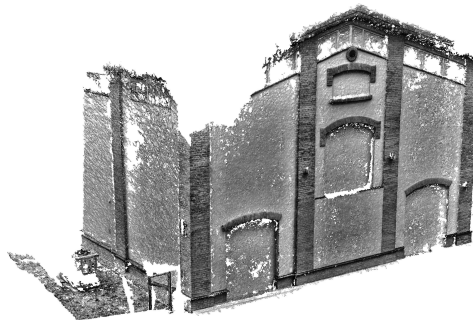
Fig. 12. Reconstruction performed with the use of images after adaptive histogram equalizing.
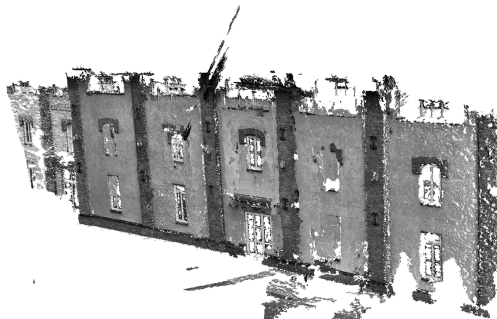
Fig. 13. Reconstruction performed with the use of images after exact histogram matching.

tion of corresponding points of the mentioned photograph and photos of neighbouring ones would improve the final result of the reconstruction.

7. Conclusion and outlook

3D photogrammetric reconstruction using unprocessed photos does not give satisfactory results. The article proposed and verified several methods of image pre-processing based on histogram analysis: conversion to grayscale, histogram stretching, histogram equalizing, adaptive histogram equalizing, and exact histogram matching. It is not possible to evidently answer which algorithm is the best, as it depends mainly on the analyzed case and the specific object. It was shown that for the analyzed cases, a significant improvement in the quality of reconstruction resulted in the use of methods: AHE and EHM. Further research in this direction is necessary, in particular regarding the extension of the scope of the analyzed cases to other types of objects and the use of different 3D reconstruction algorithms.

References

[1] J. Byrne, D.F. Laefer, E. O'Keeffe. Maximizing feature detection in aerial unmanned aerial vehicle datasets. *Journal of Applied Remote Sensing*, **11**(2), 025015, 2017, doi: 10.1117/1.JRS.11.025015.

[2] M. Cali, R. Ambu. Advanced 3D photogrammetric surface reconstruction of extensive objects by UAV camera image acquisition. *Sensors*, **18**(9): 2815, 17 pages, 2018, doi: 10.3390/s18092815.

[3] D. Coltuc, P. Bolon, J.-M. Chassery. Exact histogram specification. *IEEE Transcations on Image Processing*, **15**(5): 1143–1152, 2006.

[4] T. Jebara, A. Azarbayenjani, A. Pentland. 3D structure from 2D motion. *IEEE Signal Processing Magazine*, **16**(3): 66–84, 1999.

[5] N.D. McKay, J. Besl. A method for registration of 3-D shapes. *IEEE Transactions on Pattern Analysis and Machine Intelligence*, **14**(2): 239–256, 1992.

[6] S.M. Pizer *et al.* Adaptive histogram equalization and its variations. *Computer Vision, Graphics, and Image Processing*, **39**: 355–368, 1987.

[7] A. Semechko. Exact histogram specification and equalization of grayscale images. *GitHub*, https://www.github.com/AntonSemechko/exact_histogram, retrieved July 2, 2019.

[8] K. Zuiderveld, Contrast limited adaptive histogram equalization. In: P.S. Heckbert [Ed.], *Graphics Gems IV*, pp. 474–485, Academic Press, 1994.